

An extreme distortion of the Van Allen belt arising from the 'Hallowe'en' solar storm in 2003

D. N. Baker¹, S. G. Kanekal¹, X. Li¹, S. P. Monk¹, J. Goldstein² & J. L. Burch²

¹Laboratory for Atmospheric and Space Physics, University of Colorado, 1234 Innovation Drive, Boulder, Colorado 80303-7814, USA

²Southwest Research Institute, PO Drawer 28510, San Antonio, Texas 78284, USA

The Earth's radiation belts—also known as the Van Allen belts¹—contain high-energy electrons trapped on magnetic field lines^{2,3}. The centre of the outer belt is usually 20,000–25,000 km from Earth. The region between the belts is normally devoid of particles^{2–4}, and is accordingly favoured as a location for spacecraft operation because of the benign environment⁵. Here we report that the outer Van Allen belt was compressed dramatically by a solar storm known as the 'Hallowe'en storm' of 2003. From 1 to 10 November, the outer belt had its centre only ~10,000 km from Earth's equatorial surface, and the plasmasphere was similarly displaced inwards. The region between the belts became the location of high particle radiation intensity. This remarkable deformation of the entire magnetosphere implies surprisingly powerful acceleration and loss processes deep within the magnetosphere.

Sunspot group number 484 appeared on the east limb of the Sun's disk on 18 October 2003. As it and concurrent sunspot groups 486 and 488 rotated across the visible solar surface during the subsequent two to three weeks, the Sun produced spectacular enhancements of solar X-rays ('flares'), solar energetic particles, and, ultimately, some of the largest geomagnetic storms on record⁶. The interplanetary shock waves and coronal mass ejections launched by the Sun reached Earth's vicinity in time periods as short as one day, and produced dramatic effects in near-Earth space. In striking Earth's outer magnetic envelope (the magnetosphere), the high-speed solar disturbances compressed, distorted and enhanced the Van Allen belts. Figure 1a shows that there is a high degree of electron flux variability on daily, monthly and solar-cycle timescales^{7,8}. It is also clear that the maximum flux of energetic electrons does not occur at the time of highest sunspot number (2000–01), but rather in the declining phase (for example, 1994–95) of solar activity⁹. The period of October–November 2003 was a period of exceptional radiation belt variability.

Figure 1b demonstrates the remarkable degree to which the radiation belt electrons were displaced inwards towards the Earth in 2003 by the Hallowe'en storms after day of year (DOY) ~300. In fact, the data show that the normal peak of electron fluxes around $L = 4.0$ that was seen before (and well after) the Hallowe'en storm period was displaced far inward to $L \approx 2.5$ for a period of at least two weeks (see Fig. 1 legend for a definition of L). The normal slot region—the region between the belts, typically devoid of high-energy electrons^{3,4,10}—was filled with electrons for several weeks (from DOY ≈ 300 to DOY ≈ 340). Such an intense and long-lasting slot-filling event was not previously seen in the long run of SAMPEX satellite electron flux data (Fig. 1a). Note, also, from Fig. 1b that the inner zone ($1 \leq L \leq 2$) was filled with high-energy electrons to a degree not seen from 1992 to 2003, and that this has persisted to the present day (see also refs 11–13).

We find evidence that the great distortion and displacement of the outer radiation belt during and following the Hallowe'en storm was closely associated with a major reduction of the Earth's plasmasphere. The plasmasphere is the region of cold, relatively dense ionized gas (mostly protons and helium ions) that resides on the magnetic field lines close to the Earth¹⁴. It is understood that the

plasmasphere is threaded by magnetic flux tubes that are persistently 'closed', so that plasma from the Earth's ionosphere has filled the flux tubes and reached a near-equilibrium state along the entire dipole-like field line¹⁵. The outer boundary of the plasmasphere—known as the 'plasmopause'—can act to refract, and hence trap, electromagnetic waves propagating in the whistler mode¹⁶. Such confined waves in the plasmasphere strongly scatter trapped electrons into the atmospheric 'loss cone', causing the electrons to be 'precipitated' into the Earth's upper atmosphere¹⁷. Such precipitated electrons are removed from the magnetosphere permanently. It is generally believed that the radiation belt slot region (described above) is due to such strong scattering and loss of electrons near the plasmopause caused by strong wave-particle interactions^{16,17}.

The Imager for Magnetopause-to-Aurora Global Exploration (IMAGE) spacecraft¹⁸ makes it possible to view directly the physical extent of the plasmasphere by imaging the extreme ultraviolet (EUV) emissions from He⁺ (at 30.4 nm wavelength) within the plasmasphere¹⁹. With its high inclination and highly elliptical ($1,000 \times 46,000$ km altitude) orbit, IMAGE is able to view the Earth's plasma environs for extended periods¹⁸. Figure 2 (top row) shows that surrounding the Earth in each frame is a green-to-white 'cloud' that is due to the EUV light scattered by the He⁺ resident in the plasmasphere. Careful analysis^{19,20} allows the EUV images to be used to determine the outer edge of the plasmasphere—that is, the plasmopause.

The lower row of Fig. 2 shows the inferred plasmopause locations (in local time); they generally delineate very well the equatorial extent of the plasmasphere²⁰. Before the storm, on 28 October (leftmost panel), the plasmopause radius was between about 4 and 5 Earth radii ($4\text{--}5 R_E$). During the storm, on 31 October (second panel from the left), the plasmopause radius was inside $2 R_E$, and at some longitudes was at $1.5 R_E$. Such an extremely small plasmasphere only occurs during the strongest geomagnetic storms¹⁹, and the plasmopause shrinkage of the Hallowe'en 2003 storm is the most pronounced yet identified in the IMAGE data set.

Using available IMAGE data (as shown in Fig. 2), we have determined the plasmopause locations throughout late October and into mid-November 2003. The minimum L -value for this boundary in Fig. 1c shows that the plasmopause often tracks rather well with the inner extent of the electron radiation belt population measured by SAMPEX. In other words, the IMAGE/EUV data show a generally close correspondence (for the analysed period) between the inner edge of the outer Van Allen belt and the measured plasmopause location. It is widely accepted that the inner edge of the outer Van Allen belt should correspond rather closely to the plasmopause location¹⁶. Our data for the (post) Hallowe'en storm period show this to very much be true. Figure 1d emphasizes the point that the electron fluxes in the normal slot region ($L \approx 2.5$) were considerably higher in early November 2003 than were the fluxes in the normal 'heart' of the outer zone ($L \approx 4.0$).

Figure 3a shows schematically the radiation belt and plasmasphere under typical conditions. Under these normal circumstances, the outer radiation belt extends quite far from the Earth with its maximum intensity occurring at $\sim 4\text{--}5 R_E$ geocentric distance. The plasmasphere extends outward to $3\text{--}4 R_E$ geocentric distance. As shown in Fig. 3b, we find during (and following) the Hallowe'en 2003 storm that the plasmasphere was greatly contracted inward towards the Earth and remained in a very reduced state for many days. Concurrently, the Van Allen belt was also re-established very far inwards and the highest electron intensities were seen at $2\text{--}3 R_E$ geocentric distance.

An event of such magnitude and extent as the October–November 2003 storms provides a unique opportunity to study the acceleration, transport and loss of energetic particles in Earth's magnetosphere. In many ways, the whole state of the Earth's radiation belts was altered in a very short time by the Hallowe'en

storms. On the other hand, the dramatically altered particle fluxes during the storm had very long-lasting consequences.

An important point to note (as shown in Fig. 1) is that the immediate consequence of solar effluents hitting Earth's magnetosphere (on ~31 October 2003) was to deplete the radiation belts at almost all L -values. Then, in the subsequent day or two the radiation belt electron fluxes were regenerated to remarkably high levels. However, this regenerated population of electrons was formed in a wholly unexpected location—the normal slot region, where few electrons can ordinarily survive for any extended period. The powerful acceleration of electrons that had to occur over DOY ≈ 305 –315 was associated with very strong wave activity measured

both in space by the Polar spacecraft²¹ and on the Earth's surface by ground-based magnetometers (I. Mann, personal communication). Thus, we would expect that waves in the ultra-low frequency (ULF) range could drive rapid radial diffusion of electrons (hence accelerating the particles)²². However, it is also possible that strong 'chorus' emissions (in the whistler mode) or even electromagnetic ion cyclotron (EMIC) waves could locally heat and accelerate electrons to very high energies^{23,24} in the $L = 2$ –3 range under these exceptional conditions.

We emphasize that losses of the radiation belt electrons can be well studied by such a dramatic and sharply defined set of events as the Hallowe'en storm. As we have shown here, the inner extent of the 'new' radiation belt electron population at $2 \leq L \leq 3$ corresponds quite closely to the outward extent of the plasmasphere. Thus, even under the conditions of extreme distortion of the inner magnetosphere, it seems that strong local acceleration plus wave-particle scattering and loss near the plasmapause must determine where the outer belt electrons can persist^{16,17}.

On the basis of the exponential decay of electron fluxes seen in November 2003 at $L \approx 2.5$ (as shown here in Fig. 1d), we can estimate the 'e-folding' lifetime of 2–6 MeV electrons from the following equation: $J(E = 2\text{--}6 \text{ MeV}) = K \exp(-t/t_0)$ where J is electron flux, K is a proportionality constant, and t_0 is the 'lifetime' of the electrons against precipitation loss (or radial diffusion away from $L = 2.5$). From a simple fitting procedure, we find that from 3 to 20 November, $t_0 \approx 4.6$ days. Following the other major storm enhancement that occurred on 20 November 2003, there was another decay over the interval 25 November to 20 December 2003. This led to $t_0 \approx 2.9$ days. Thus, the 'active' acceleration and decay episodes produced within the inner magnetosphere by the Sun's output gives us a direct measure of the loss lifetimes of electrons in the inner magnetosphere¹⁶.

A final point to note about losses is that many electrons obviously passed through the normal slot-region 'barrier' following the Hallowe'en storm and entered the inner zone ($1 \leq L \leq 2$) region (see Fig. 1b, c). These electrons constitute a new, powerful, population of very energetic electrons in the inner zone that have not been present there since the remnants of the March 1991 storm died away^{11–13}.

The presence of very energetic electrons in the Earth's magnetosphere constitutes a 'space weather' hazard to spacecraft operating in near-Earth space⁵. The Hallowe'en storms generated large fluxes

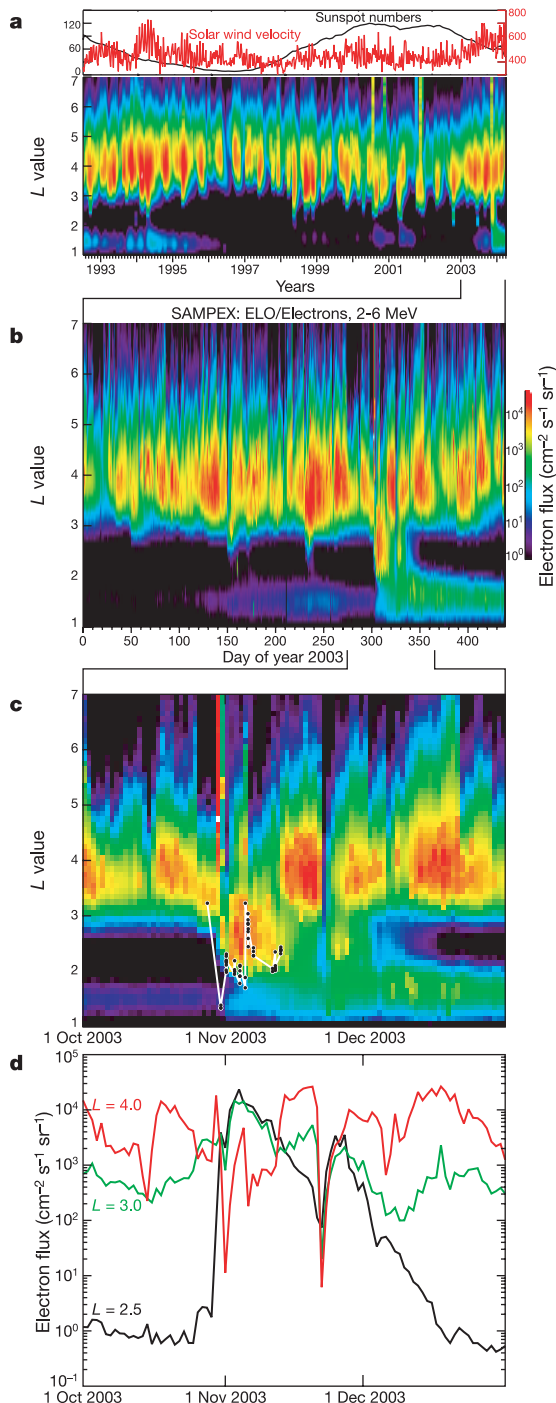


Figure 1 Energetic electron data from a low-altitude Earth-orbiting spacecraft showing both a long historical record of the Van Allen radiation belts and the specific effects of the 2003 Hallowe'en storm. **a**, Flux of 2–6 MeV electrons measured by the Solar, Anomalous, and Magnetospheric Particle Explorer (SAMPEX)⁷ from 6 July 1992 to March 2004. Data are coded according to the colour bar to the right. Vertical axis is the L -shell parameter, which is effectively the distance in Earth radii at which a magnetic field line crosses the magnetic equatorial plane. The small upper panel shows (in black) the yearly-averaged solar sunspot number (SSN) and (in red) the weekly-averaged solar wind speed (V_{sw}) measured upstream of the Earth⁸. This panel demonstrates intense electron acceleration events (due to high-speed solar wind) in 1993–95 for $3 \leq L \leq 5$. During sunspot minimum (1996), there were significant electron events only briefly around the spring and autumn equinoxes⁹. A weak, but persistent, feature in the inner zone died away throughout 1992 and 1993; it intensified in 1994. This may, in part, be related to the 'new' radiation belt created during the March 1991 storm^{11,12}. **b**, Detailed SAMPEX electron data (daily-averaged) for 2003 and early 2004 showing the shifted position of the outer Van Allen zone and the filling of the slot region. **c**, SAMPEX data for the period 1 October to 31 December 2003. The broken line superimposed on the SAMPEX data shows the plasmapause as measured by IMAGE. **d**, Electron fluxes in the energy range $2 \leq E \leq 6$ MeV for three L -values (red: $L = 4.0$; green: $L = 3.0$; and black: $L = 2.5$) for the period 1 October to 31 December 2003. The energetic electron intensities at

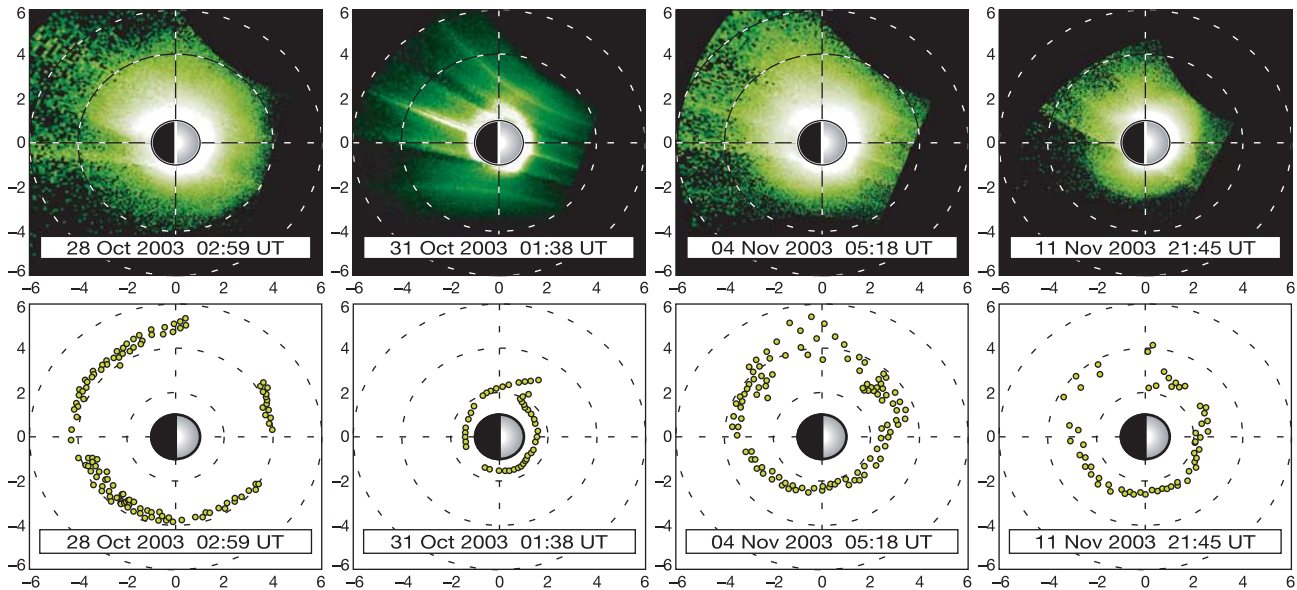


Figure 2 Extreme ultraviolet (EUV) images of the Earth's plasmasphere during late October and early November 2003. Images in the top row range in time from before the Halloween storm (28 October 2003) to well after the main storm period (11 November 2003). The Earth position is illustrated in each frame, showing the sunward and night sides by each central shaded half-circle. The effects of the Halloween storm are clearly evident in the series of plasmasphere snapshots. Another effect of the storm is in the quality of the images obtained by the EUV instrument. During the storm, an abundance of energetic particles led to radiation penetrating into the EUV cameras, creating noise in the

images. In the 31 October plasmasphere image, curved diagonal streaks of noise due to this effect are evident, cutting across the image from top-left to bottom-right. In the several days after the storm (4 November and 11 November, right two panels), the plasmasphere recovered from its extreme shrinkage, as plasma from the Earth's ionosphere gradually leaked out into space and repopulated the plasmaspheric flux tubes. The lower row of panels shows the plasmopause locations inferred at each time from each corresponding image on the top. The plasmopause positions are plotted in the equatorial x - y plane where the scale in each frame is in terms of Earth radii ($1 R_E = 6,372$ km).

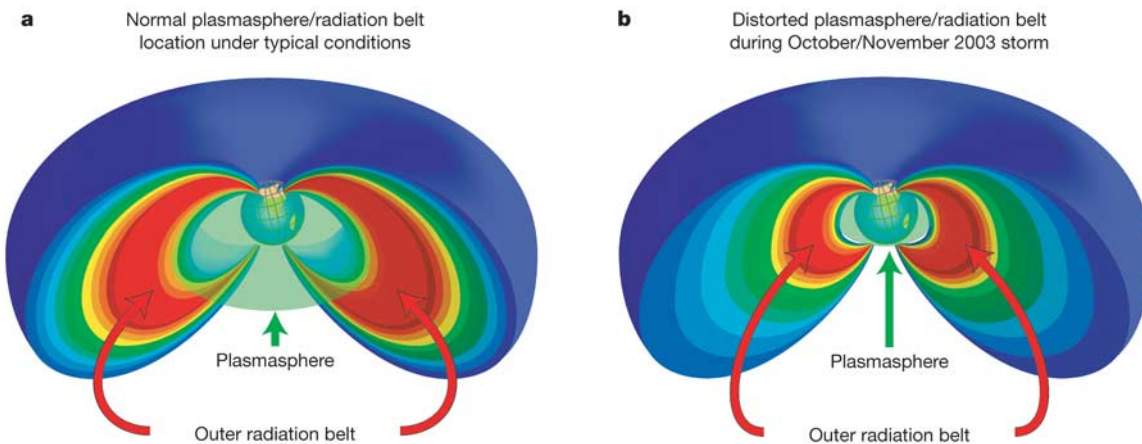


Figure 3 Diagrams of the three-dimensional view of the Earth's outer radiation belt and its relationship to the plasmasphere. **a**, A schematic diagram showing the Earth, the outer radiation belt, and the normal plasmaspheric location. **b**, Similar to **a** but showing the highly contracted plasmasphere and greatly distorted radiation belt location during the

Halloween storm period. These cutaway diagrams show the highest electron fluxes as red and the lowest fluxes as blue. The radiation belt is a 'doughnut' or torus-shaped entity. The Earth is portrayed at the centre. Also shown, as a translucent green torus towards the centre in each part of the figure, is the plasmasphere.

of solar energetic particles as well as the high fluxes of radiation belt electrons reported here. The combination of solar and magnetospheric particles produced a whole host of 'anomalies' in technological systems during October–November 2003²⁵. In fact, a few outright spacecraft failures and other significant losses were directly attributable to this space weather. We have shown that a set of events (as occurred with the Halloween storm) substantially changed the radiation environment at $L \leq 3$, and very hostile space weather suddenly developed in a region that is normally quiescent. So future models and design strategies need to take account of possible extreme events, such as occurred in October–November 2003. □

Received 6 July; accepted 12 October 2004; doi:10.1038/nature03116.

1. Van Allen, J. A. in *Discovery of the Magnetosphere* (eds Gillmor, C. S. & Spreiter, J. R.) 235–251 (Vol. 7, History of Geophysics, American Geophysical Union, Washington DC, 1997).
2. Vette, J. I. *The AE-8 Trapped Electron Model Environment* (NSSDC WDC-A-R&S 91-24, NASA Goddard Space Flight Center, Greenbelt, Maryland, 1991).
3. Brautigam, D. H., Gussenhoven, M. S. & Mullen, E. G. Quasi-static model of outer zone electrons. *IEEE Trans. Nucl. Sci.* **39**, 1797–1803 (1992).
4. Lyons, L. R. & Thorne, R. M. Equilibrium structure of radiation belt electrons. *J. Geophys. Res.* **78** (13), 2142–2149 (1973).
5. Baker, D. N. How to cope with space weather. *Science* **297**, 1486–1487 (2002).
6. Lopez, R. E., Baker, D. N. & Allen, J. H. Sun unleashes Halloween storm. *Eos* **85**, 105, 108 (2004).
7. Baker, D. N. *et al.* An overview of the Solar Anomalous, and Magnetospheric Particle Explorer (SAMPEX) mission. *IEEE Trans. Geosci. Remote Sens.* **31**, 531–541 (1993).

8. Li, X. *et al.* The predictability of the magnetosphere and space weather. *Eos* **84**, 361, 369–370 (2003).
9. Baker, D. N., Kanekal, S. G., Pulkkinen, T. I. & Blake, J. B. Equinoctial and solstitial averages of magnetospheric relativistic electrons: A strong semiannual modulation. *Geophys. Res. Lett.* **26**, 3193–3196 (1999).
10. Blake, J. B. *et al.* New high temporal and spatial resolution measurements by SAMPEX of the precipitation of relativistic electrons. *Adv. Space Res.* **18**, 171–177 (1996).
11. Looper, M. D. *et al.* Observations of remnants of the ultrarelativistic electrons injected by the strong SSC of 24 March 1991. *Geophys. Res. Lett.* **21**, 2079–2082 (1994).
12. Li, X. *et al.* Simulation of the prompt energization and transport of radiation particles during the March 23, 1991 SSC. *Geophys. Res. Lett.* **20**, 2423–2426 (1993).
13. Li, X. in *Proc. 6th Int. Conf. on Substorms (ICS6)* (ed. Winglee, R. M.) 305–311 (Univ. Washington Press, Seattle, Washington, 2000).
14. Carpenter, D. L. & Park, C. G. What ionospheric workers should know about the plasmapause/plasmasphere. *Rev. Geophys.* **11**, 133–154 (1973).
15. Grebowky, J. M. Model study of plasmapause motion. *J. Geophys. Res.* **75**, 4329–4333 (1970).
16. Thorne, R. M., Smith, E. J., Burton, R. K. & Holzer, R. E. Plasmaspheric hiss. *J. Geophys. Res.* **78** (10), 1581–1598 (1973).
17. Lorentzen, K. R., Blake, J. B., Inan, U. S. & Bortnik, J. Observations of relativistic electron microbursts in association with VLF chorus. *J. Geophys. Res.* **A 106**, 6017–6027 (2001).
18. Burch, J. L. *et al.* Views of the Earth's magnetosphere with the IMAGE satellite. *Science* **291**, 619–624 (2001).
19. Sandel, B. R., Goldstein, J., Gallagher, D. L. & Spasojevic, M. Extreme ultraviolet imager observations of the structure and dynamics of the plasmasphere. *Space Sci. Rev.* **109**, 25–46 (2003).
20. Goldstein, J. *et al.* Simultaneous remote sensing and *in situ* observations of plasmaspheric drainage plumes. *J. Geophys. Res.* **109**, doi:10.1029/2003JA010281 (2004).
21. Russell, C. T., Cartwright, M. & Kanekal, S. The formation of the inner zone trapped radiation belt. *Adv. Space Res.* (in the press).
22. Liu, W. W., Rostoker, G. & Baker, D. N. Internal acceleration of relativistic electrons by large-amplitude ULF pulsations. *J. Geophys. Res.* **104**, 17391–17407 (1999).
23. Summers, D., Thorne, R. M. & Xiao, F. Relativistic theory of wave-particle resonant diffusion with application to electron acceleration in the magnetosphere. *J. Geophys. Res.* **A 103**, 20487–20500 (1998).
24. Summers, D. & Thorne, R. M. Relativistic electron pitch-angle scattering by electromagnetic ion cyclotron waves during geomagnetic storms. *J. Geophys. Res.* **108**, doi:10.1029/2002JA009489 (2003).
25. Webb, D. F. & Allen, J. H. Spacecraft and ground anomalies related to the October–November 2003 solar activity. *Space Weather* **2**, doi:10.1029/2004SW000075 (2004).

Acknowledgements This work was supported by NASA. We thank members of the SAMPEX and IMAGE science teams for data and discussions.

Competing interests statement The authors declare that they have no competing financial interests.

Correspondence and requests for materials should be addressed to D.N.B. (daniel.baker@lasp.colorado.edu).

Hall-effect evolution across a heavy-fermion quantum critical point

S. Paschen¹, T. Lühmann¹, S. Wirth¹, P. Gegenwart¹, O. Trovarelli¹, G. Geibel¹, F. Steglich¹, P. Coleman² & Q. Si³

¹Max Planck Institute for Chemical Physics of Solids, Nöthnitzer Straße 40, D-01187 Dresden, Germany

²Center for Materials Theory, Department of Physics and Astronomy, Rutgers University, Piscataway, New Jersey 08855, USA

³Department of Physics and Astronomy, Rice University, Houston, Texas 77005-1892, USA

A quantum critical point (QCP) develops in a material at absolute zero when a new form of order smoothly emerges in its ground state. QCPs are of great current interest because of their singular ability to influence the finite temperature properties of materials. Recently, heavy-fermion metals have played a key role in the study of antiferromagnetic QCPs. To accommodate the heavy electrons, the Fermi surface of the heavy-fermion paramagnet is larger than that of an antiferromagnet^{1–3}. An important unsolved question is whether the Fermi surface transformation at the QCP develops gradually, as expected if the magnetism is of spin-density-wave (SDW) type^{4,5}, or suddenly, as expected if the heavy electrons are abruptly localized by magnetism^{6–8}. Here we report measurements of the low-temperature Hall coefficient

(R_H)—a measure of the Fermi surface volume—in the heavy-fermion metal YbRh_2Si_2 upon field-tuning it from an antiferromagnetic to a paramagnetic state. R_H undergoes an increasingly rapid change near the QCP as the temperature is lowered, extrapolating to a sudden jump in the zero temperature limit. We interpret these results in terms of a collapse of the large Fermi surface and of the heavy-fermion state itself precisely at the QCP.

The compound YbRh_2Si_2 investigated here appears to be one of the best suited heavy-fermion metals known in which to study the evolution of the Hall effect across a QCP. Magnetic susceptibility and specific heat indicate that this compound orders antiferromagnetically via a second-order phase transition at very low temperatures (Néel temperature $T_N = 70$ mK)⁹. The antiferromagnetic nature of the transition is supported by NMR data¹⁰. Neutron scattering experiments to directly detect the magnetic order are not available to date, presumably owing to the smallness of the ordered moment¹¹. T_N is continuously suppressed down to the lowest experimentally accessed temperatures by application of a small magnetic field B_c ($B_{1c} \approx 0.7$ T for a field along the magnetically hard c axis, $B_{2c} \approx 60$ mT for a field within the easy tetragonal plane)¹². In addition, isothermal magnetostriction measurements indicate that the transition remains of second order down to at least 15 mK (ref. 13). Although a change from second to first order at even lower temperatures can, of course, not be strictly ruled out, the non-Fermi liquid behaviour observed for three decades of temperature ($10 \text{ mK} < T < 10 \text{ K}$)¹² is best described within a quantum critical picture. The use of tiny fields permits one to reversibly access the QCP without the introduction of additional disorder and without altering the character of the underlying zero-field transition¹⁴. Moreover, unlike the case of several other heavy-fermion compounds¹⁵ (and the high- T_c superconductors), the QCP is not hidden by superconductivity. This is in spite of the high quality of the YbRh_2Si_2 single crystals investigated here (residual resistivities of $\sim 1 \mu\Omega \text{ cm}$, ref. 12). The scaling analysis of the thermodynamic and dynamical properties (specific heat, magnetic susceptibility, electrical resistivity) suggests¹² that the field-induced QCP in YbRh_2Si_2 is of local^{6–8} rather than of itinerant^{4,5} type, similar to the doping-induced QCP in $\text{CeCu}_{6-x}\text{Au}_x$ (ref. 6). Hall-effect measurements may be used to access a static electronic property, namely the Fermi surface volume, for which clear-cut theoretical predictions exist for different types of QCP^{7,8,16}. The study presented here is, to our knowledge, the first systematic Hall-effect measurement at a heavy-fermion QCP.

The Hall effect, usually a rather complex quantity, appears to be surprisingly simple here, both in vanishingly small and in finite magnetic fields. Outside the quantum critical region, the Hall resistivity is linear in field, resembling the behaviour of simple metals. Furthermore, our analysis of the temperature-dependent Hall coefficient in terms of the anomalous Hall effect (Fig. 1a, Methods, and refs 17 and 18) reveals that the low-temperature (below about 1 K) Hall coefficient is dominated by its normal contribution. These features imply that the low-temperature Hall coefficient can be used, to a good approximation, as a measure of the Fermi surface volume. In the absence of photoemission and de Haas–van Alphen studies (the latter presumably never being available because of the very low critical magnetic field), and of electronic bandstructure calculations, this is, so far, the only information on the Fermi surface volume of YbRh_2Si_2 . At zero magnetic field, the data measured at the lowest temperatures tend to saturate at the value of the normal Hall coefficient extracted from the data between 7 K and room temperature (Fig. 1a). This indicates that, at $B = 0$, the Fermi surface volume is the same at the lowest temperatures as it is at high temperatures. Thus, even though there is evidence for the onset of Kondo screening at approximately 20 K (refs 9 and 12) and for surprisingly large effective quasiparticle masses in the antiferromagnetically ordered state close to the QCP¹², the local moments do not, at the lowest temperatures and at $B = 0$